

Application of Fluorescence Microscopy for Investigation of Cellular Distribution of Dinuclear Platinum Anticancer Drugs

Ganna V. Kalayda,[†] Guofang Zhang,[†] Tsion Abraham,[‡] Hans J. Tanke,^{*,‡} and Jan Reedijk^{*,†}

Leiden Institute of Chemistry, Gorlaeus Laboratories, Leiden University, P.O. Box 9502, 2300 RA Leiden, The Netherlands, and Laboratory for Cytochemistry and Cytometry, Department of Molecular Cell Biology, Leiden University Medical Center, Wassenaarseweg 72, 2333 AL Leiden, The Netherlands

Received March 9, 2005

The dinuclear platinum complexes with aliphatic diamines [*cis*-Pt(NH₃)₂Cl]₂(μ-H₂N(CH₂)₆-NH₂)(NO₃)₂ (1,1/c,c) and [*trans*-Pt(NH₃)₂Cl]₂(μ-H₂N(CH₂)₄NH₂)(NO₃)₂ (1,1/t,t), which are known to be highly active in vitro against several cancer cell lines, have been modified with a fluorogenic reporter (carboxyfluorescein diacetate, CFDA) and a hapten (dinitrophenyl, DNP). These labeled complexes have been designed for fluorescence microscopy investigation of cellular pathways of promising dinuclear platinum anticancer drugs and present the first example of labeling biologically active dinuclear platinum complexes with a fluorescent reporter. The modified compounds interact with a guanine model base similarly to the label-free parent complexes. The uptake of the complexes with a fluorescent label and the respective unlabeled complexes in the U2-OS human osteosarcoma cell line and its cisplatin-resistant derivative, U2-OS/Pt cell line has been investigated. Cellular processing of the CFDA- and DNP-modified dinuclear platinum complexes in U2-OS and U2-OS/Pt cells has been studied.

Introduction

Dinuclear and polynuclear cationic platinum complexes present a new, promising class of anticancer drugs. A number of these complexes exhibit high activity against various types of tumors, and their cytotoxic profiles are often different from the profiles of cisplatin and its analogues.^{1–4} Many polynuclear platinum complexes overcome intrinsic and acquired resistance to cisplatin.^{5–7} Their positive charge provides high affinity for the presumed cellular target of antitumor drugs, i.e. nuclear DNA, and additional positive charge introduced in the bridging ligand appears to result in higher anticancer activity. Dinuclear platinum complexes with polyamines spermine and spermidine, and the trinuclear complex BBR3464 that now undergo clinical trials, serve as good examples.^{7–10}

Different cytotoxic profiles of dinuclear platinum complexes and their ability to overcome cisplatin resistance are believed to result from structurally different DNA adducts formed by these compounds.^{5,11–13} However, uptake and intracellular transport also play an important role in the mechanism of action of platinum-based drugs and in the mechanism of resistance.^{14–17} Cellular organelles are known to participate in transport of platinum anticancer complexes^{18–21} and have been recently found to contribute to cisplatin resistance and cross-resistance.²⁰ Thus, investigation of cellular distribution of platinum antitumor drugs might help to better understand their mechanism of action on an intracellular level. This knowledge is of great importance for the development of new tumor-specific anti-

cancer agents because the sensitivity of cancer cells to a given drug varies significantly between tumor cell types.

Digital fluorescence microscopy enables visualization of fluorescent compounds in cells. A big advantage of this method is that it allows observation of the cells in a living state. Fluorescence microscopy has been widely used to study cellular distribution of various organic drugs^{22–24} and has been successfully applied to platinum complexes.^{18–20} Because most dinuclear platinum anticancer complexes are not intrinsically fluorescent, they need to be modified with a fluorescent or fluorogenic tag in order to visualize them in tumor cells.

This paper describes the synthesis and cellular processing of new dinuclear platinum complexes modified with a fluorogenic reporter or a hapten (Figure 1), which have been designed as model compounds for investigation of cellular distribution and processing of promising antitumor dinuclear platinum complexes. Approaches of labeling dinuclear platinum complexes of *cis* and *trans* geometries with fluorogenic tags are presented. The pharmacokinetics properties of the labeled model complexes and their parent dinuclear complexes are compared. Cellular processing of the new labeled dinuclear platinum complexes in cancer cells is described.

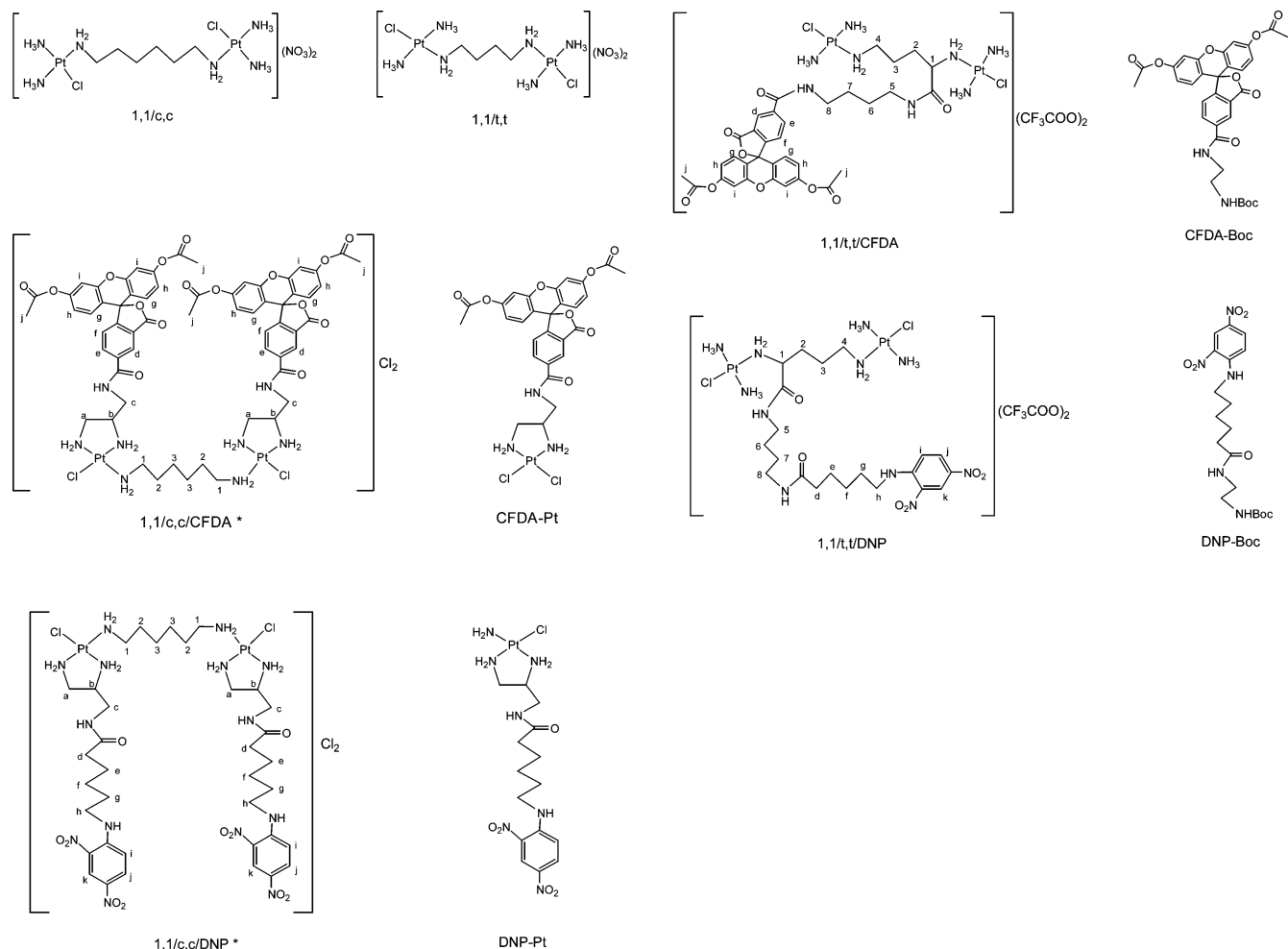
Results

Synthesis. The labeled dinuclear platinum complexes of *cis* geometry 1,1/c,c/CFDA and 1,1/c,c/DNP (Figure 1), where 1,1/c,c/CFDA is [bis{(1-(5-(and 6)-carboxyfluorescein-diacylate-aminomethyl)-1,2-ethylenediamine)chloroplatinum(II)}(μ-1,6-hexanediamine)] chloride and 1,1/c,c/DNP is [bis{(1-(2,4-dinitrophenyl-hexanoic-aminomethylene)-1,2-ethylenediamine)chloroplatinum(II)}(μ-1,6-hexanediamine)] chloride, were designed similarly to the previously described mononuclear complexes CFDA-Pt and DNP-Pt,¹⁸ which represent labeled

* To whom correspondence should be addressed. For H.J.T.: phone, +31715276190; fax, +31715276180; e-mail: h.j.tanke@lumc.nl. For J.R.: phone, +31715274459; fax, +31715274671; e-mail: reedijk@chem.leidenuniv.nl.

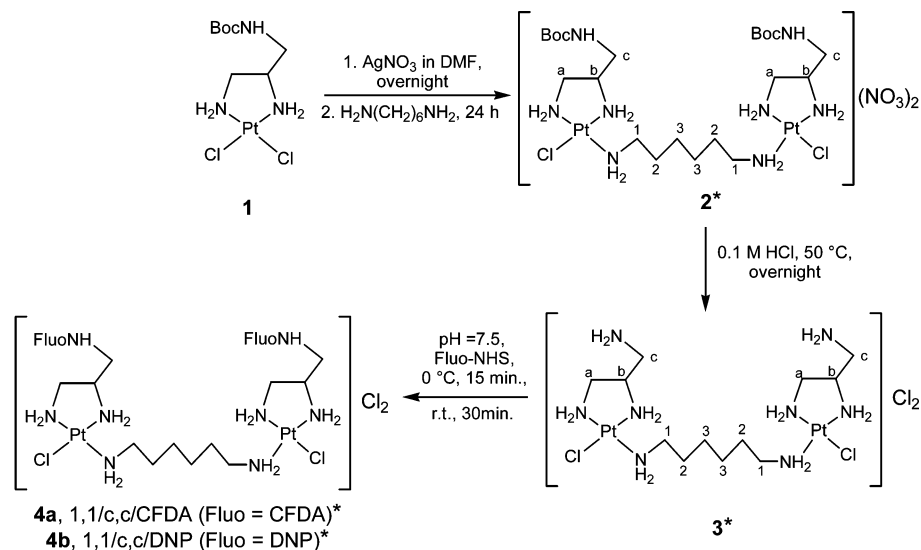
[†] Leiden University.

[‡] Leiden University Medical Center.



* mixture of three geometric isomers

Figure 1. Schematic representation of the labeled dinuclear platinum complexes 1,1/c,c/CFDA, 1,1/c,c/DNP, 1,1/t,t/CFDA, and 1,1/t,t/DNP, the parent dinuclear complexes 1,1/c,c and 1,1/t,t, and the compounds used in the control experiments, CFDA-Pt, DNP-Pt, CFDA-Boc, and DNP-Boc.



* mixture of three geometric isomers

Figure 2. Schematic representation of the synthetic route used for preparation of 1,1/c,c/CFDA and 1,1/c,c/DNP.

analogues of cisplatin. A standard method for preparation of dinuclear platinum complexes was used to

synthesize the dinuclear precursor **2** (Figure 2). It has been obtained in a good yield and probably represents

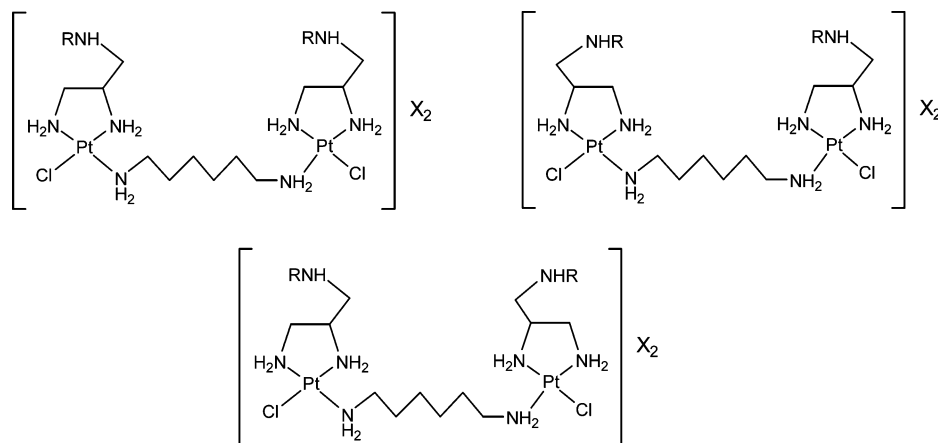


Figure 3. Schematic representation of the geometric isomers of **2** (R = Boc, X = NO₃), **3** (R = H, X = Cl), **4a** (R = CFDA, X = Cl), and **4b** (R = DNP, X = Cl).

a mixture of the three isomers shown in Figure 3. Moreover, each of these geometric isomers consists of three diastereomers (*R,R*; *R,S* (*S,R*); *S,S*). Subsequent removal of the Boc group did not affect the dinuclear platinum moiety and resulted in the formation of **3** with negligible amounts of impurities. The labeled compounds **4a** and **4b** were obtained by coupling of **3** with the active esters of CFDA and DNP probes, respectively. Compounds **2**, **3**, **4a**, and **4b** most likely represent mixtures of isomeric complexes. However, ¹H NMR spectra did not allow us to distinguish among different isomers for any of the compounds because the chemical shifts of the protons have been found to be the same, independent of the ligand location around platinum. Since all isomers **4a** (and also all isomers **4b**) represent equally good fluorogenic models of 1,1/*c,c*, separation was not felt to be necessary and the compounds were used in biological studies as mixtures of isomers. The purity of the compounds overall was high, as verified with HPLC/ESI-MS and elemental analysis (as located in Supporting Information) and confirmed by ¹H and ¹⁹⁵Pt NMR. Any impurities are so small that they are unlikely to affect the observed biological data. The relatively large deviation from the theoretical values for the carbon analyses of **4a** and **4b** is ascribed to the presence of the solvent in the samples and will have no influence on the biological data.

For structural reasons, the dinuclear platinum complexes of *trans* geometry could not be designed in a similar fashion. Considering the stability of the resulting labeled complexes and possible synthetic routes for their preparation, introducing the label in the linker between two platinum atoms appeared to be the best option. The synthesis of 1,1/*t,t*/CFDA and 1,1/*t,t*/DNP (Figure 1), where 1,1/*t,t*/CFDA is [bis{*trans*-diamminechloroplatinum(II)}{*μ*-(2,5-diamino-*N*-(4-(5-(and 6)-carboxy-fluorescein-diacetate-amino)butyl)valeramide)}] trifluoroacetate and 1,1/*t,t*/DNP is [bis{*trans*-diamminechloroplatinum(II)}{*μ*-(2,5-diamino-*N*-(4-(2,4-dinitrophenylhexanoic-amino)butyl)valeramide)}] trifluoroacetate, is schematically presented in Figure 4. Ligand **8** was prepared in three steps from ornithine hydrochloride, similar to the method previously described by some of us.²⁵ First, the amino groups of ornithine were protected by reaction with ethyl trifluoroacetate. This ensured that no side reactions would take place at the next step of coupling of amine **5** to the ornithine moiety. Attaching

amine **5** would provide an opportunity to introduce a label (CFDA or DNP) relatively far away from the dinuclear platinum moiety, minimizing possible steric hindrance. Subsequently, the trifluoroacetyl protection group was cleaved off by NaOH, while the acid-labile *tert*-butoxycarbonyl group was not affected. In such a way, two amino groups would be available for platination, and the Boc-protected amino group could later be replaced with the fluorogenic reporter or the hapten. Platination of ligand **8** was performed with [*trans*-Pt-(NH₃)₂Cl(dmef)](NO₃) species according to the standard procedure for the synthesis of dinuclear platinum complexes. Subsequent removal of the Boc group and reaction with an active ester of CFDA and DNP label yielded **11a** (1,1/*t,t*/CFDA) and **11b** (1,1/*t,t*/DNP), respectively, which were purified by HPLC. LC/ESI-MS analysis and ¹H and ¹⁹⁵Pt NMR spectrometry confirmed the purity of the products.

Reaction with a Guanine Model Base. The complexes modified with the DNP hapten (1,1/*c,c*/DNP and 1,1/*t,t*/DNP) were allowed to react with 9-ethylguanine (9EtG) at 310 K to investigate how the labeled complexes interact with nucleobases. The parent compounds 1,1/*c,c* and 1,1/*t,t* were studied as references. For all four complexes, the signal of the H8 proton of 9EtG at 7.88 ppm decreases in intensity during the course of the reaction, while the signals of H8 protons of the products increase in intensity, indicating platination of the nucleobase. Only one signal of the product was observed in the case of a 1,1/*c,c*/DNP mixture of isomers, indicating that all of them interact with a guanine model base identically. Interestingly, the H8 signals of the 9EtG adducts of 1,1/*c,c*/DNP and 1,1/*c,c* appear at 8.30 and 8.31 ppm, respectively, and the H8 signals of the 9EtG adducts of both 1,1/*t,t*/DNP and 1,1/*t,t* appear at 8.27 ppm. This suggests similar conformation of the nucleobase in the labeled and label-deprived 9EtG adducts.

The pH titration of the 9EtG adducts of the labeled and parent complexes was performed. The plots of the chemical shifts of H8 proton as a function of pH are presented in Figure 5 and clearly show the absence of the (de)protonation process at the N7 atom of 9EtG at low pH, which indicates platinum binding at this position.^{26,27} At the same time, (de)protonation at N1 was observed providing additional confirmation for platinum coordination at N7. Moreover, pH titration curves for the 9EtG adduct of 1,1/*t,t* and its DNP-labeled

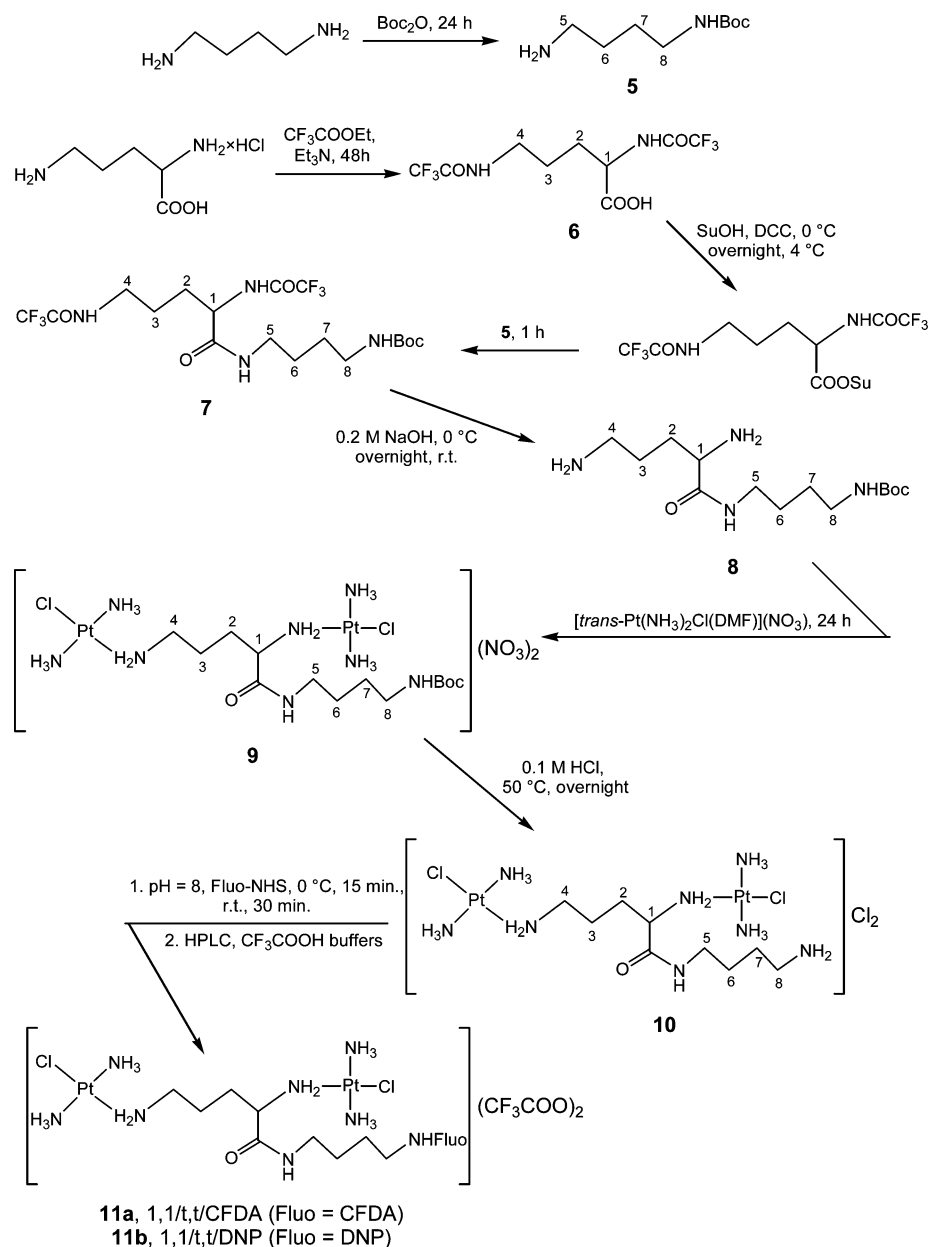


Figure 4. Schematic representation of the synthetic route used for preparation of 1,1/t,t/CFDA and 1,1/t,t/DNP.

counterpart almost coincide, again confirming similar conformation of the guanine molecule in both adducts. A deviation of the pH titration curve for the 1,1/c,c/DNP adduct with 9EtG from that for the 1,1/c,c adduct can be explained by the influence of the chelating ligands present in the labeled complex.

Thus, these data suggest that the DNP-labeled constructs interact with nucleobases in a way similar to that of the label-free parent compounds.

Uptake of the Complexes by U2-OS and U2-OS/Pt Osteosarcoma Cells. To compare some of the pharmacokinetics properties of the labeled and parent complexes, their uptake by U2-OS and U2-OS/Pt cells was studied by means of measuring platinum concentration inside the cells after 30 min, 2 h, and 24 h of incubation.

Figure 6 shows that for all compounds platinum accumulation in both cell lines increases as a function of incubation time. Uptake of cisplatin and the fluorescent labeled model complexes, CFDA-Pt and DNP-Pt,

is lower in the resistant cell line than in the sensitive one at any period of incubation. This is in agreement with previously reported data, which show decreased cisplatin accumulation in the U2-OS/Pt cell line compared to its sensitive counterpart.²⁸ In contrast, no great difference in platinum accumulation between U2-OS and U2-OS/Pt cell lines was found for any of dinuclear platinum complexes. Thus, the labeled derivatives of cisplatin and dinuclear platinum complexes mimic the behavior of the parent compounds. Nevertheless, some differences in cellular uptake between the labeled and the label-deprived complexes were observed. Accumulation of 1,1/c,c/CFDA and 1,1/c,c/DNP is significantly higher than that of the parent complex, 1,1/c,c, most likely because of the presence of two lipophilic reporters per molecule (Figure 6b). As is clear from parts a and c of Figure 6, introducing one label per molecule (as in the case of CFDA-Pt or 1,1/t,t/CFDA) does not have a significant influence on the accumulation of the complexes in the cells.

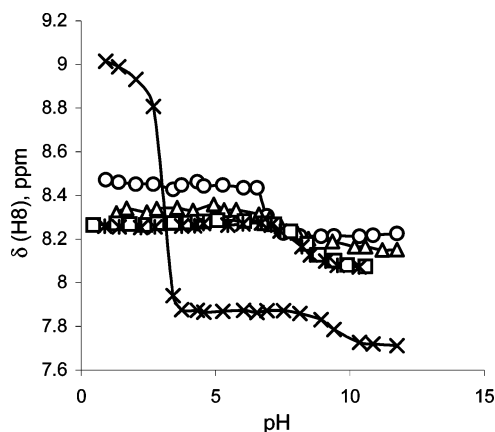


Figure 5. Plots of the chemical shift (δ , ppm) of the H8 resonance vs pH for the 9EtG adducts of 1,1/c,c/DNP (○) and 1,1/c,c (△), for the 9EtG adducts of 1,1/t,t/DNP (*) and 1,1/t,t (□), and for the free 9EtG ligand (×). pH titrations were performed in 0.1 M NaClO₄/D₂O solutions at 298 K.

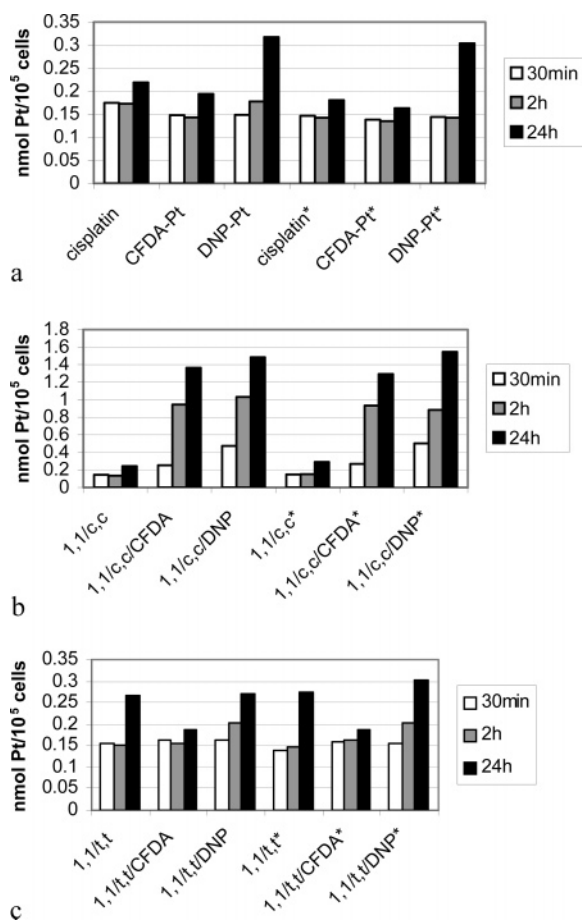


Figure 6. Platinum concentration in U2-OS and U2-OS/Pt human osteosarcoma cells after 30 min, 2 h, and 24 h of incubation with the labeled and label-free dinuclear platinum complexes. The values represent the average of the measurements.

Fluorescence Studies in Living Cells. The CFDA-labeled dinuclear complexes were used to investigate cellular processing of potential dinuclear platinum antitumor drugs in U2-OS human osteosarcoma cells. CFDA is a fluorogenic label, which is readily taken up by cells. In the cytoplasm, the acetate esters of CFDA are cleaved by cellular esterases, yielding a fluorescent moiety.¹⁸ CFDA is known to have a negligible impact

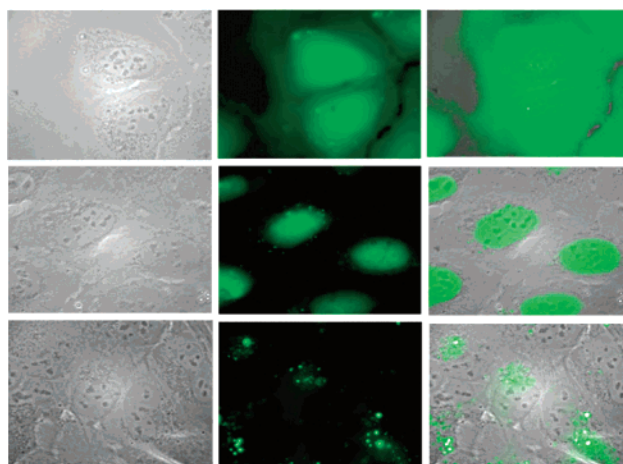


Figure 7. Cellular processing of 1,1/c,c/CFDA in U2-OS human osteosarcoma cells. The images taken 15 min after internalization are presented in the top row. Images 1 h after internalization are in the middle row, and images 24 h after internalization are in the bottom row. Phase contrast images of the cells at these time points are presented on the left, corresponding fluorescence images are in the middle, and superimposed images are on the right.

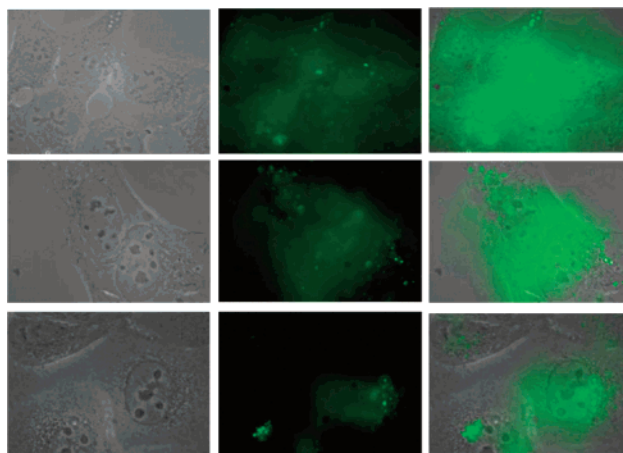


Figure 8. Cellular processing of 1,1/t,t/CFDA in U2-OS human osteosarcoma cells. The images taken 15 min after internalization are presented in the top row. Images 1 h after internalization are in the middle row, and images 24 h after internalization are in the bottom row. Phase-contrast images of the cells at these time points are presented on the left, corresponding fluorescence images are in the middle, and superimposed images are on the right.

on cell viability.^{29,30} The cells were incubated with 1,1/c,c/CFDA and 1,1/t,t/CFDA and then observed live using digital fluorescence microscopy. The mononuclear fluorescent-labeled complex CFDA-Pt and metal-free CFDA-Boc were used in control experiments (images not shown). The phase contrast and fluorescence images of the cells after incubation with 1,1/c,c/CFDA and 1,1/t,t/CFDA are presented in Figures 7 and 8, respectively.

As is clear from Figures 7 and 8, cellular distribution of the dinuclear platinum complexes of cis and trans geometries is quite similar. Both compounds quickly enter the cells; several minutes after internalization, the fluorescence can already be seen throughout the entire cell. One hour later, fluorescence is mainly concentrated in the nucleus. Interaction of the platinum complexes with genomic DNA probably occurs at this stage.

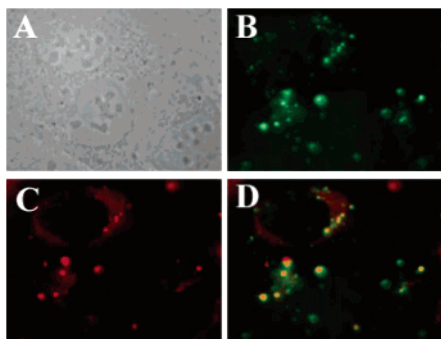


Figure 9. Combination of 1,1/c,CFDA accumulation 24 h after internalization and staining with Bodipy-TR-ceramide (a Golgi specific dye) in living U2-OS cells: (A) phase-contrast image of living U2-OS cells; (B) 1,1/c,CFDA (green) fluorescence in these cells 24 h after internalization; (C) staining of the Golgi complex with Bodipy-TR-ceramide (red); (D) superimposed representation of the images of 1,1/c,CFDA (green) and Bodipy-TR-ceramide (red).

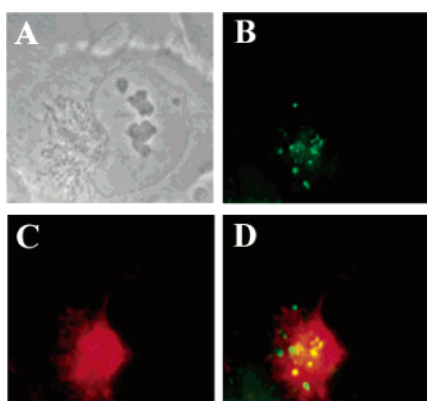


Figure 10. Combination of 1,1/t,CFDA accumulation 24 h after internalization and staining with Bodipy-TR-ceramide (a Golgi specific probe) in living U2-OS cells: (A) phase-contrast image of living U2-OS cells; (B) 1,1/t,CFDA (green) fluorescence in these cells 24 h after internalization; (C) staining of the Golgi complex with Bodipy-TR-ceramide (red); (D) superimposed representation of the images of 1,1/t,CFDA (green) and Bodipy-TR-ceramide (red).

Besides, fluorescence of the trans complex was also observed in the cytoplasm, next to the nucleus. Four to five hours after internalization, the fluorescence in the nucleus becomes weaker and punctuate staining in the area of cytoplasm close to the nucleus is detected (data not shown). The same cellular distribution pattern is observed 24 h after internalization, with the signal in the nucleus being very weak. On the basis of spatial considerations, we supposed the cytoplasmic region close to the nucleus, where the fluorescent complexes accumulate, to be the Golgi complex. To verify this hypothesis, a colocalization experiment with a Golgi-specific fluorescent dye was performed. At 24 h after internalization, Bodipy-Texas red (TR)-ceramide was added, and the cells were incubated for 20 min. The images of the cells incubated with 1,1/c,CFDA and the Bodipy-TR-ceramide are shown in Figure 9, and images of cells after incubation with 1,1/t,CFDA and Bodipy-TR-ceramide are presented in Figure 10. Green fluorescence of the cis and trans complexes can be seen in Figures 9B and 10B, respectively, and red fluorescence of Bodipy-TR-ceramide is shown in Figures 9C and 10C. The superimposed images (Figures 9D and 10D) clearly

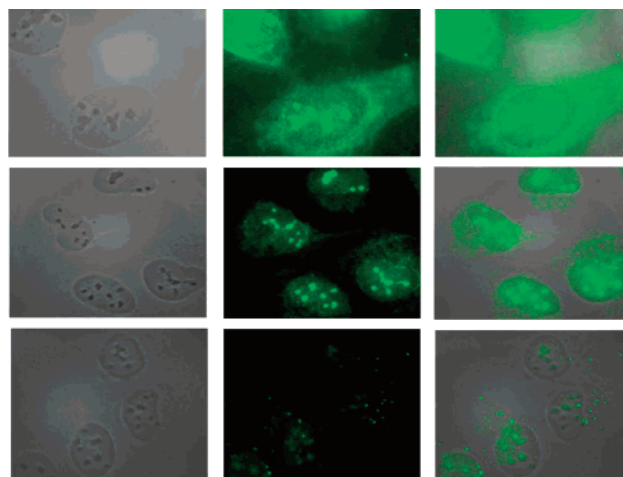


Figure 11. Cellular processing of 1,1/c,DNP in U2-OS human osteosarcoma cells. The images of the cells fixed 15 min after internalization are presented in the top row, those of the cells fixed 1 h after internalization are in the middle row, and images of the cells fixed 24 h after internalization are in the bottom row. Phase-contrast images of the cells at these time points are presented on the left, corresponding fluorescence images are in the middle, and superimposed images are on the right.

show that the fluorescence of 1,1/c,CFDA and 1,1/t,CFDA is localized in the Golgi complex.

Cellular processing of CFDA-Pt and CFDA-Boc, which were used in control experiments, was found to be similar to the previously described processing by Molenaar et al.¹⁸ As is clear from the results of the control experiment, cellular processing of the fluorescent labeled dinuclear complexes is very similar to that of CFDA-Pt. CFDA-Boc is quickly taken up by the cells, equally distributed throughout the cell, and excreted within 5–6 h, showing no specific localization in the nucleus or cellular organelles. This confirms that the results of fluorescence observations for the CFDA-labeled dinuclear platinum complexes are induced by a platinum moiety and not by CFDA label itself.

To verify that the observed results are label-independent, cellular processing of the structurally similar DNP-modified complexes 1,1/c,DNP and 1,1/t,DNP in U2-OS cells was studied. DNP was chosen as a well-known hapten, which is easily visualized with DNP-specific antibodies. The cells were incubated with the DNP constructs under the same conditions as in the case of the CFDA-labeled complexes. For the observations, the cells were fixed at different time points after incubation, and DNP was visualized by indirect immunofluorescence. The images of the cells incubated with 1,1/c,DNP and 1,1/t,DNP are presented in Figures 11 and 12, respectively. Both cis and trans DNP constructs show accumulation in the nucleus 1 h after internalization. Localized accumulation in a cytoplasmic area close to the nucleus has been observed 24 h after internalization with 1,1/c,DNP and 1,1/t,DNP, similar to the case of CFDA constructs. No specific accumulation in U2-OS cells was observed after incubation with DNP-Boc (images not shown). Thus, cellular distribution of DNP-labeled dinuclear complexes is not different from that of structurally similar CFDA-labeled counterparts. These observations and the results of cellular processing experiments with platinum-free CFDA-Boc and DNP-

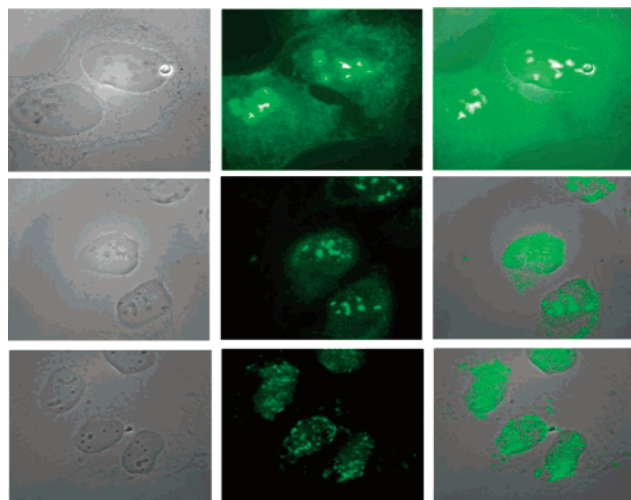


Figure 12. Cellular processing of 1,1/t,t/DNP in U2-OS human osteosarcoma cells. The images of the cells fixed 15 min after internalization are presented in the top row, those of the cells fixed 1 h after internalization are in the middle row, and images of the cells fixed 24 h after internalization are in the bottom row. Phase-contrast images of the cells at these time points are presented on the left, corresponding fluorescence images are in the middle, and superimposed images are on the right.

Table 1. In Vitro Cytotoxicity Assay of 1,1/c,c, 1,1/t,t, Cisplatin and Their Fluorescent-Labeled Derivatives on U2-OS Human Osteosarcoma Cell Line and Cisplatin-Resistant U2-OS/Pt Cell Line

complex	IC ₅₀ (μM)		RF ^a
	U2-OS	U2-OS/Pt	
1,1/c,c/CFDA	>50	>50	na ^b
1,1/c,c/DNP	>50	>50	na ^b
1,1/c,c	5.1	6.1	1.2
1,1/t,t/CFDA	>50	>50	na ^b
1,1/t,t/DNP	>50	>50	na ^b
1,1/t,t	75.1	38.6	0.5
CFDA-Pt	>50	>50	na ^b
DNP-Pt	>50	>50	na ^b
cisplatin	2.9	7.3	2.5

^a RF = the relative ratio of IC₅₀ values in both cell lines ((U2-OS/Pt)/U2-OS). ^b na = not available.

Boc prove that the observed cellular distribution pattern is induced by a dinuclear platinum moiety.

Cellular processing of the labeled dinuclear platinum complexes in the cisplatin-resistant U2-OS/Pt cell line was also investigated. No differences in cellular distribution of the compounds between sensitive and resistant cells were found (images not shown). The same observation was previously made in the case of the mononuclear complex CFDA-Pt¹⁸ and was confirmed in our control experiment.

In Vitro Cytotoxicity Assay in U2-OS and U2-OS/Pt Cell Lines. The cytotoxicity of the labeled and label-free parent dinuclear platinum complexes has been evaluated in U2-OS human osteosarcoma cell line and its cisplatin-resistant derivative U2-OS/Pt cell line. The results are given in Table 1. The labeled complexes are poorly water-soluble and were dissolved in dimethylformamide for the biological tests. Unfortunately, the toxicity of the solvent at the desired compound concentration did not allow us to precisely determine the IC₅₀ values for the labeled complexes.

As is clear from Table 1, the dinuclear platinum complex of cis geometry, 1,1/c,c, is as active as cisplatin, whereas the trans complex 1,1/t,t is significantly less cytotoxic in the U2-OS osteosarcoma cell line. Such low activity of the trans complex is surprising because the trinuclear platinum complex of trans geometry, BBR3464, has been reported to be much more active than cisplatin in this cell line.^{28,31} Both dinuclear platinum complexes show no cross-resistance with cisplatin. Interestingly, the U2-OS/Pt cell line has a lower (2.5-fold) degree of resistance than found earlier by Perego et al. (6-fold).²⁸

Discussion

Labeling dinuclear platinum complexes with a fluorescent or fluorogenic tag gives us an excellent opportunity to study cellular pathways of these promising anticancer drugs using fluorescence microscopy. Time-lapse digital fluorescence microscopy allows us to follow the processing of compounds in the cells growing at 37 °C in vitro. Investigation of cellular distribution of intrinsically fluorescent organic antitumor drugs helped to reveal the role of cellular organelles, such as lysosomes, Golgi apparatus, and mitochondria, in transport and detoxification of the drugs,^{22,32} as well as involvement of organelles in resistance mechanisms.^{24,33} Fluorescence microscopy was also applied to study cellular behavior of biologically active platinum complexes. To visualize the latter in cells, antibodies against Pt-DNA adducts have been developed.³⁴ A cisplatin analogue labeled with a fluorogenic tag had been synthesized earlier, and investigation of its cellular processing revealed involvement of the Golgi apparatus in the transport of platinum complexes.¹⁸ Cellular distribution of the dinuclear platinum complexes with fluorescent anthraquinones has also been studied and provided new insights in the resistance mechanisms in A2780 human ovarian carcinoma cells.²⁰

The platinum complexes modified with the CFDA moiety, which are described in this work, present the first example of labeling dinuclear platinum complexes with a fluorescent or fluorogenic tag. A label can be introduced in the bridging ligand as well as in the side chain. The former approach is especially useful in the case of trans complexes. The labeled complexes interact with a guanine model base similarly to the parent compounds, indicating that modification with a fluorogenic tag does not significantly influence binding of the dinuclear platinum complexes to nucleobases. Cellular uptake of the labeled compounds is affected by the presence of a lipophilic fluorescent moiety. It has been suggested by Hall et al.³⁵ that CFDA-labeled complexes diffuse in and out of the cells and intracellular compartments at a greater rate compared to the parent compounds. Our results show that cellular accumulation of the complexes containing two reporters per molecule is indeed significantly higher. Nevertheless, the modified complexes appear to mimic the uptake of the parent compounds. Accumulation of cisplatin and its modified analogues is lower in cisplatin-resistant cells than in sensitive cells, which is in agreement with the resistance profile of the U2-OS/Pt cell line.²⁸ The uptake of the dinuclear platinum complexes (1,1/c,c and 1,1/t,t) and the respective model complexes with a fluorescent probe by sensitive and resistant osteosarcoma cells is the

same, which reflects the lack of cross-resistance of 1,1/c,c and 1,1/t,t with cisplatin in U2-OS/Pt cells. Thus, it can be concluded that the CFDA- and DNP-labeled compounds represent good models for the respective parent dinuclear platinum complexes.

Cellular processing of the labeled dinuclear complexes in U2-OS human osteosarcoma cells appeared to be similar to the previously described cellular distribution of the mononuclear complex CFDA-Pt.¹⁸ Using two different labels (CFDA and DNP) and the control experiments with CFDA-Boc and DNP-Boc ensures that the observed results are induced by a dinuclear platinum moiety. Interestingly, no differences in cellular processing between the complexes with cis and trans geometries were found. In contrast to cis-configured dinuclear platinum complexes, complexes with the trans configuration are known to lose their bridging ligand upon interaction with glutathione.^{36,37} Therefore, the labeled complexes 1,1/t,t/CFDA and 1,1/t,t/DNP could possibly release their fluorescent linking ligand inside the cell, resulting in a different cellular distribution pattern. It must be noted, however, that platinum-free controls (CFDA-Boc and DNP-Boc) are processed by cells in a different way compared to the dinuclear complexes. This finding indicates that the release of the bridging ligand from 1,1/t,t/CFDA and 1,1/t,t/DNP in U2-OS cells is negligible, most probably because of the relatively low GSH content in this cell line.²⁸

The dinuclear complexes enter the cell rapidly, within minutes. Given their positive charge, this finding indicates active mechanism of uptake for dinuclear complexes. The results of cellular uptake measurements presented in this paper, as well as some earlier uptake studies,³⁸ show that dinuclear platinum complexes accumulate in the cells to the same extent or better than cisplatin. Within 1 h, they accumulate in the nucleus where they bind to nuclear DNA. The fluorescence intensity in the nucleus weakens with time, suggesting that the labeled complexes are partially removed. In fact, only a fraction of the complexes binds to DNA, and as already mentioned, they are likely to diffuse out of the nucleus. However, removal of platinum-DNA lesions by nuclear excision repair proteins, as a part of DNA repair process, also contributes to the overall decrease of platinum concentration in the nucleus. Several hours after internalization, the dinuclear platinum complexes are localized in the Golgi complex, and this localization is still observed 24 h after internalization. Accumulation in the Golgi apparatus in sensitive and resistant U2-OS cell lines has been reported not only for the mononuclear CFDA-labeled analogue of cisplatin¹⁸ but also for the dinuclear platinum complexes with fluorescent anthraquinones.²¹ There is mounting evidence indicating that the Golgi plays an important role in drug transport.^{23,24,39} The Golgi complex is probably a site where platinum complexes accumulate before being excreted via exocytosis. The platinum compounds might be exocytosed as a part of general mechanism by which secretory proteins are transported to the external cell surface. P-glycoprotein, which is known to be involved in the efflux of various drugs, is localized on the luminal side of Golgi stack membranes in U2-OS cells.⁴⁰ However, it is not certain whether P-glycoprotein participates in the efflux of platinum complexes.

No involvement of lysosomes in the exocytosis of platinum complexes, as reported for other cell lines,^{19,41,42} was observed. Also, no accumulation in mitochondria, as described for other types of cancer cells,^{43–46} was found. Apparently, the cellular distribution pattern may vary significantly between different cancer cell lines. This has been recently confirmed by investigation of cellular processing of the dinuclear platinum complexes with anthraquinones in different cell lines.²¹

No differences in cellular processing of the labeled dinuclear platinum complexes in U2-OS and U2-OS/Pt cells were observed, which is completely in agreement with the lack of cross-resistance of both 1,1/c,c and 1,1/t,t with cisplatin. In fact, the U2-OS/Pt cell line has a relatively low (2.5-fold) degree of resistance. This provides an explanation for the similar cellular distribution of CFDA-Pt in sensitive and resistant osteosarcoma cells as reported by Molenaar et al.¹⁸

Concluding Remarks

Dinuclear platinum complexes modified with a fluorescent or fluorogenic reporter present a useful tool for the investigation of cellular distribution of these promising antitumor drugs. Fluorescence microscopy studies of their cellular trafficking might provide new insights in the mechanism of action of this class of anticancer compounds. Given that many dinuclear platinum complexes overcome cisplatin resistance, labeled complexes might help to elucidate resistance mechanisms. Using cell lines with different resistance profiles is especially interesting because it might reveal new specific features of a given cell type.

Experimental Section

Instruments. ¹H and ¹⁹⁵Pt NMR spectra were recorded on a Bruker DPX 300 MHz spectrometer with a 5 mm multi-nucleus probe. The temperature was kept constant by a variable-temperature unit. ¹H and ¹⁹⁵Pt chemical shifts were referenced to TSP and Na₂PtCl₆ ($\delta = 0$ ppm), respectively. C, H, and N analyses were performed by the microanalytical laboratory of Leiden Institute of Chemistry, Leiden University, The Netherlands.

The mass spectroscopic measurements were performed on a Finnigan Aqa mass spectrometer equipped with an electrospray interface ionization source. Sample solutions were introduced in the ESI source using an HPLC autosampler and an acetonitrile/water (50/50) mixture as an eluent running at 0.2 mL/min.

LC/ESI-MS experiments were carried out on a Alltima 3 μ m C18 reversed-phase column (150 mm \times 4.6 mm) with a flow rate of 1 mL/min, sample load of 10–50 μ L (1 mg/mL), and the following gradient conditions: 95% eluent B for 2 min, then from 95% eluent B to 70% eluent B in 20 min, and subsequently from 70% eluent B to 10% eluent B in 8 min (eluent A, acetonitrile with 0.1% CF₃COOH; eluent B, 0.1% aqueous solution of CF₃COOH). After that, the column flow is split. One part flows through the UV detector (254 nm). The other part (0.2 mL/min) is directed to the Finnigan Aqa mass detector operating in electrospray mode.

The samples were purified with reversed-phase chromatography using an Alltima 5 μ m C18 column (250 mm \times 10 mm) with a flow rate of 4 mL/min and a repetitive sample load of 500 μ L using the following gradient: 95% eluent B for 2.4 min, then from 95% eluent B to 70% eluent B in 23.6 min, and subsequently from 70% eluent B to 10% eluent B in 9.5 min (eluent A, acetonitrile with 0.1% CF₃COOH; eluent B, 0.1%

aqueous solution of CF₃COOH). Fractions were collected and analyzed by mass spectrometry, and the desired fraction was lyophilized.

Synthesis. Materials. CFDA-Pt, DNP-Pt, CFDA-Boc, DNP-Boc, and {1-(*tert*-butoxycarbonylaminomethyl)-1,2-ethylenediamine}dichloroplatinum(II) (**1**) were synthesized as described by Molenaar et al.¹⁸ The *trans*-Pt(NH₃)₂Cl₂ compound was prepared according to the literature procedure.⁴⁷ [{*cis*-Pt(NH₃)₂Cl]₂(μ-H₂N(CH₂)₆NH₂)](NO₃)₂ (1,1/*c,c*) and [{*trans*-Pt(NH₃)₂Cl]₂(μ-H₂N(CH₂)₄NH₂)](NO₃)₂ (1,1/*t,t*) were synthesized as previously described.^{48–50} K₂PtCl₄ was obtained from Johnson & Matthey. Silver nitrate was purchased from Fisher Scientific Nederland. Ornithine hydrochloride, ethyl trifluoroacetate, and dicyclohexylcarbodiimide (DCC) were purchased from Aldrich. Triethylamine, 1,4-butanediamine, 1,6-hexanediamine, and di-*tert*-butyl dicarbonate were ordered from Acros. *N*-Hydroxysuccinimide (SuOH) was purchased from Nova Biochem. 5-(and 6-)-Carboxyfluorescein diacetate succinimidyl ester (5(6)-CFDA SE) and 6-(2,4-dinitrophenyl)amino hexanoic acid succinimidyl ester (DNP-X SE) were obtained from Molecular Probes Europe BV, Leiden, The Netherlands. 9-Ethylguanine was purchased from Sigma.

Bis{[1-(*tert*-butoxycarbonylaminomethyl)-1,2-ethylenediamine]chloroplatinum(II)}(μ-1,6-hexanediamine) Nitrate (2**).** To a solution of 90.4 mg (0.2 mmol) of **1** in 4.8 mL of dimethylformamide (DMF) was added portionwise over 2 h in the dark a solution of 33 mg (0.19 mmol) of AgNO₃ in 1.2 mL of DMF, and the resulting solution was stirred for 5 h in the dark. The white precipitate of AgCl was then filtered off, and a solution of 10.4 mg (0.09 mmol) of 1,6-hexanediamine in 1 mL of DMF was added to the filtrate. The resulting solution was stirred overnight in the dark and then evaporated to dryness. The residue was dissolved in 1 mL of methanol. The product was precipitated with 20 mL of ether, stirred with ether for several hours to remove traces of DMF, filtered, and dried in air. Yield: 57 mg (53%). Anal. (C₂₂H₅₄N₁₀O₁₀Cl₂Pt₂). C: calcd, 24.47; found, 24.31. H: calcd, 5.04; found, 4.28. N: calcd, 12.97; found, 12.89. ¹H NMR (D₂O): δ 3.37 (m, 2H, H_c), 3.02 (m, 1H, H_b), 2.87 (m, 1H, H_a), 2.70 (m, 2H, H₁), 2.57 (m, 1H, H_a), 1.68 (m, 2H, H₂), 1.45 (s, 18H, Boc), 1.39 (m, 2H, H₃). ¹⁹⁵Pt NMR (D₂O): δ -2585.

Bis{[1-(aminomethyl)-1,2-ethylenediamine]chloroplatinum(II)}(μ-1,6-hexanediamine) Chloride (3**).** An amount of 13.4 mg (1.24 × 10⁻² mmol) of **2** was dissolved in 1.5 mL of 100 mM hydrochloric acid and heated at 50 °C overnight in the dark. This resulted in the formation of a solution of **3**, which was directly used for the synthesis of compounds **4a** and **4b**. Successful removal of the Boc group under these conditions was proven by taking an aliquot and performing a pH titration monitored by ¹H NMR. The resonance of H_c protons showed pH dependence as expected for the protonation/deprotonation of the free primary amine. ¹H NMR (D₂O, pH 7.1): δ 3.27 (m, 2H, H_c), 3.01 (m, 1H, H_b), 2.85 (m, 1H, H_a), 2.75 (m, 3H, H₁ + H_a), 2.57 (m, 1H, H_a), 1.73 (m, 2H, H₂), 1.43 (m, 2H, H₃).

Bis{[1-(5-(and 6-)carboxyfluorescein-diacetate-aminomethyl)-1,2-ethylenediamine]chloroplatinum(II)}(μ-1,6-hexanediamine) Chloride (1,1/*c,c*/CFDA, **4a).** A solution of **3** obtained as described above was neutralized with 2 M NaOH until pH 7.5 was attained. Then it was cooled to 0 °C, and a solution of 12.7 mg of 5(6)-CFDA SE (2.28 × 10⁻² mmol) in 1.5 mL of DMF was added dropwise. The resulting solution was stirred first for 20 min at 0 °C and then for 30 min more at room temperature. The solvents were subsequently removed in vacuo. The residue was stirred vigorously with 4 mL of ice-cold water, filtered off, and washed three times with 4 mL of ice-cold water, three times with 4 mL of ethanol, and three times with diethyl ether. The sample was dried in vacuo. Yield: 7 mg (33%). Anal. (C₆₂H₆₆N₈O₁₆Cl₄Pt₂). C: calcd, 43.52; found, 44.8. H: calcd, 3.89; found, 3.81. N: calcd, 6.55; found, 6.24. ¹H NMR (DMF-*d*₇): δ 8.38 (m, 1H, H_d), 8.02 (under DMF-HCO, 1H, H_e), 7.70 (d, 1H, H_f), 7.32 (m, 2H, H_g), 7.03 (m, 4H, H₁ + H_b), 3.45 (under H₂O, 2H, H_c), 3.13 (m, 1H, H_b), 2.76 (under DMF-CH₃, 4H, H₁ + H_a), 2.33

(s, 6H, H_j), 1.68 (m, 2H, H₂), 1.27 (m, 2H, H₃). ¹⁹⁵Pt NMR (DMF-*d*₇): δ -2590.

Bis{[1-(2,4-dinitrophenylhexanoic-aminomethylene)-1,2-ethylenediamine]chloroplatinum(II)}(μ-1,6-hexanediamine) Chloride (1,1/*c,c*/DNP, **4b).** A solution of **3** obtained as described above was neutralized with 2 M NaOH until pH 7.5 was attained. Then it was cooled to 0 °C, and a solution of 9.0 mg of DNP-X SE (2.28 × 10⁻² mmol) in 1.5 mL of DMF was added dropwise. The resulting solution was stirred first for 20 min at 0 °C and then for 30 min more at room temperature. The solvents were subsequently removed in vacuo. The residue was stirred vigorously with 4 mL of ice-cold water, filtered off, and washed three times with 4 mL of ice-cold water, three times with 4 mL of ethanol, and three times with diethyl ether. The sample was dried in vacuo. Yield: 6 mg (35%). Anal. (C₃₆H₆₄N₁₄O₁₀Cl₄Pt₂). C: calcd, 31.22; found, 32.22. H: calcd, 4.66; found, 3.86. N: calcd, 14.16; found, 14.30. ¹H NMR (DMF-*d*₇): δ 8.96 (s, 1H, H_k), 8.35 (d, 1H, H_j), 7.37 (d, 2H, H_i), 3.61 (m, 4H, H_c + H_b), 3.14 (m, 1H, H_b), 2.78 (under DMF-CH₃, 3H, H₁ + H_a), 2.63 (m, 1H, H_a), 2.29 (t, 2H, H_d), 1.78 (m, 2H, H_g), 1.69 (m, 4H, H₂ + H_e), 1.48 (m, 2H, H_f), 1.34 (m, 2H, H₃). ¹⁹⁵Pt NMR (DMF-*d*₇): δ -2600.

***N*-*tert*-Butoxycarbonyl-1,4-butanediamine (**5**).** To a solution of 7.5 g (85.08 mmol) of 1,4-butanediamine in 30 mL of dioxane, a solution of 2.4 g (11.00 mmol) of di-*tert*-butyl dicarbonate in 30 mL of dioxane was added dropwise over 1.5 h. The solution was stirred at room temperature for 22 h. The solvent was evaporated in vacuo, and 50 mL of water was added. The insoluble material was filtered off, and the filtrate was extracted with 3 × 45 mL of dichloromethane. The combined organic phase was dried over MgSO₄, filtered, and evaporated to provide the product. Yield: 1.152 g (60.12%). ¹H NMR (CDCl₃): δ 3.13 (t, 2H, H₈), 2.70 (t, 2H, H₅), 1.53 (m, 4H, H₂ + H₃), 1.47 (s, 9H, Boc).

***N,N'*-Bis(trifluoroacetyl)ornithine (**6**).** To a solution of 4 g (23.72 mmol) of ornithine hydrochloride in 120 mL of methanol were added 6.67 mL of triethylamine (47.5 mmol) and 7.05 mL (59.25 mmol) of ethyl trifluoroacetate. The resulting mixture was stirred at room temperature for 48 h, filtered, and evaporated to dryness. The white residue was dissolved in 120 mL of 1 M hydrochloric acid. After evaporation to dryness, 140 mL of ethyl acetate was added, the solution was filtered, and the filtrate was concentrated in vacuo. To the remaining solid, 120 mL of 1 M hydrochloric acid was added, and the white product was filtered off, washed with 1 M hydrochloric acid, and dried in air. Yield: 6.23 g (81.03%). Anal. (C₉H₁₀N₂O₄F₆). N: C: calcd, 33.34; found, 32.95. H: calcd, 3.11; found, 3.03. ¹H NMR (MeOH-*d*₄): δ 4.45 (m, 1H, H₁), 3.28 (m, 2H, H₄, under MeOH), 1.94 (m, 1H, H₂), 1.78 (m, 1H, H₂), 1.60 (m, 2H, H₃).

2,5-Bis(trifluoroacetyl-amino)-*N*-(4-*tert*-butoxycarbonylaminobutyl)valeramide (7**).** To a solution of 2 g (6.15 mmol) of **6** in 50 mL of tetrahydrofuran were added at 0 °C a solution of 0.7 g (6.1 mmol) of SuOH in 5 mL of tetrahydrofuran and a solution of 1.3 g of DCC (6.3 mmol) in 5 mL of tetrahydrofuran. The mixture was allowed to stand overnight at 4 °C. The insoluble material was then filtered off, and a solution of 1.152 g (6.61 mmol) of **5** in 25 mL of ethanol was added to the filtrate. The resulting solution was stirred at room temperature for 1 h, filtered, and evaporated to dryness. The residue was dissolved in 25 mL of ethylene glycol dimethyl ether, 100 mL of water was added, and the precipitated product was collected by filtration. The sample was dried in air. Yield: 2.569 g (84.22%). Anal. (C₁₈H₂₈N₄O₅F₆). C: H: calcd, 5.71; found, 5.58. N: calcd, 11.33; found, 11.14. ¹H NMR (MeOH-*d*₄): δ 4.38 (m, 1H, H₁), 3.30 (m, 2H, H₄, under MeOH), 3.20 (m, 2H, H₈), 3.03 (m, 2H, H₅), 1.75–1.85 (m, 2H, H₂), 1.55–1.64 (m, 6H, H₃ + H₆ + H₇), 1.40 (m, 9H, Boc).

2,5-Diamino-*N*-(4-*tert*-butoxycarbonylaminobutyl)valeramide (8**).** To a solution of 2.57 g (5.2 mmol) of **7** in 80 mL of methanol, 58 mL of 0.2 M NaOH (11.6 mmol) was added dropwise at 0 °C. The solution was stirred overnight at room temperature, then filtered and extracted with 5 × 35 mL of CHCl₃/MeOH (9:1). The organic phase was dried over MgSO₄,

filtered, and evaporated to provide the product. Yield: 1.57 g (99.92%). ^1H NMR ($\text{MeOH}-d_4$): δ 3.24 (m, 1H, H_1), 3.19 (m, 2H, H_8), 3.03 (m, 2H, H_4), 2.62 (m, 2H, H_5), 1.65 (m, 2H, H_2), 1.58 (m, 6H, $\text{H}_3 + \text{H}_6 + \text{H}_7$), 1.40 (m, 9H, Boc). ESI-MS: m/z 303.17 ($\text{M} + \text{H}$), 325.08 ($\text{M} + \text{Na}$).

Bis[*trans*-diamminechloroplatinum(II)]{ μ -(2,5-diamino-*N*-(4-*tert*-butoxycarbonylamino)butyl)valeramide} Nitrate (9). To a solution of 150 mg (0.50 mmol) of *trans*- $[\text{PtCl}_2(\text{NH}_3)_2]$ in 5 mL of DMF, a solution of 81 mg (0.475 mmol) of AgNO_3 in 5 mL of DMF was added. The solution was stirred in the dark overnight at room temperature. The precipitated AgCl was filtered off. To the remaining yellow filtrate, 68 mg (0.225 mmol) of ligand **8** in 3 mL of DMF was added dropwise. After the mixture was stirred in the dark for 24 h, DMF was evaporated in vacuo. The remaining solid was dissolved in a minimal amount of methanol. After that, the excess diethyl ether was added, resulting in the formation of a white precipitate. The suspension was stirred for several hours to remove DMF, and the white product was filtered off, washed with diethyl ether, and dried in air. The complex was purified by recrystallization from a mixture of ethanol and water (3:2), washed with ethanol and diethyl ether, and subsequently lyophilized. Yield: 115 mg (48%). Anal. ($\text{C}_{14}\text{H}_{42}\text{N}_{10}\text{O}_9\text{Cl}_2\text{Pt}_2$). C: calcd, 17.60; found, 17.14. H: calcd, 4.43; found, 4.32. N: calcd, 14.66; found, 15.00. ^1H NMR (D_2O): δ 3.82 (m, 1H, H_1), 3.38 (m, 2H, H_4), 3.12 (m, 2H, H_8), 2.65 (m, 2H, H_5), 1.74 (m, 2H, H_2), 1.60–1.70 (m, 6H, $\text{H}_3 + \text{H}_6 + \text{H}_7$), 1.43 (m, 9H, Boc). ^{195}Pt NMR (D_2O): δ –2401.

Bis[*trans*-diamminechloroplatinum(II)]{ μ -(2,5-diamino-*N*-(4-(5-(and 6)-carboxyfluorescein-diacetate-amino)butyl)valeramide} Trifluoroacetate (1,1/*t,t*/CFDA, 11a). A solution of 38.2 mg (0.040 mmol) of **9** in 2 mL of 0.1 M hydrochloric acid was stirred in the dark overnight at 50 °C to obtain a solution of **10**, which was directly used for the synthesis of **11a**. After this solution was neutralized to pH 8.0 with 2 M NaOH, a solution of 21.2 mg (0.038 mmol) of 5(6)-CFDA SE in 2 mL of DMF was added dropwise at 0 °C. The resulting solution was stirred at 0 °C for 15 min and then for 30 min at room temperature. The solvents were removed in vacuo, and the residue was dissolved in 2 mL of a mixture of acetonitrile and water (1:1) and purified by high-performance liquid chromatography as described above. The purified product was lyophilized and characterized by ^1H and ^{195}Pt NMR and LC/ESI-MS. Yield: 2.1 mg (3.8%). ^1H NMR (D_2O): δ 8.22 (s, 1H, H_d), 8.09 (d, 1H, H_e), 7.61 (d, 1H, H_f), 7.28 (s, 2H, H_i), 7.08 (d, 2H, H_g), 6.98 (d, 2H, H_h), 3.49 (m, 1H, H_1), 3.38 (m, 2H, H_4), 3.24 (m, 2H, H_8), 3.02 (m, 2H, H_5), 2.38 (s, 6H, H_3), 1.95–1.45 (m, 8H, $\text{H}_2 + \text{H}_3 + \text{H}_6 + \text{H}_7$). ^{195}Pt NMR (D_2O): δ –2410. Analytical HPLC coupled to MS: gradient, 95% B for 2 min, then from 95% B to 70% B in 20 min and subsequently from 70% B to 10% B in 8 min (eluent A, acetonitrile with 0.1% CF_3COOH ; eluent B, 0.1% aqueous solution of CF_3COOH); retention time 27.3 and 27.7 min; for both peaks m/z = 1287 ($\text{M} - \text{CF}_3\text{COO}$), 587 ($(\text{M} - 2\text{CF}_3\text{COO})/2$).

Bis[*trans*-diamminechloroplatinum(II)]{ μ -(2,5-diamino-*N*-(4-(2,4-dinitrophenyl)hexanoicamino)butyl)valeramide} Trifluoroacetate (1,1/*t,t*/DNP, 11b). A solution of 38.2 mg (0.040 mmol) of **9** in 2 mL of 0.1 M hydrochloric acid was stirred in the dark overnight at 50 °C to obtain a solution of **10**, which was directly used for the synthesis of **11b**. After this solution was neutralized to pH 8.0 with 2 M NaOH, a solution of 15.0 mg (0.038 mmol) of DNP-X SE in 2 mL of DMF was added dropwise at 0 °C. The resulting yellow solution was stirred at 0 °C for 15 min and subsequently for 30 min at room temperature. The solvents were removed in vacuo, and the residue was dissolved in 2 mL of the mixture of acetonitrile and water (1:1) and purified by high-performance liquid chromatography as described above. The purified product was lyophilized and characterized by ^1H and ^{195}Pt NMR and LC/ESI-MS. Yield: 2.1 mg (4.2%). ^1H NMR (D_2O): δ 9.17 (s, 1H, H_k), 8.34 (d, 1H, H_l), 7.20 (d, 1H, H_j), 3.58 (m, 3H, $\text{H}_b + \text{H}_1$), 3.26 (m, 2H, H_4), 3.19 (m, 2H, H_8), 2.71 (m, 2H, H_5), 2.27 (m, 2H, H_a), 1.73 (m, 6H, $\text{H}_c + \text{H}_g + \text{H}_2$), 1.65 (m, 6H, $\text{H}_3 + \text{H}_6 + \text{H}_7$), 1.46 (m, 2H, H_7). ^{195}Pt NMR (D_2O): δ –2430. Analytical

HPLC coupled to MS: gradient, 95% B for 2 min, then from 95% B to 70% B in 20 min and subsequently from 70% B to 10% B in 8 min (eluent A, acetonitrile with 0.1% CF_3COOH ; eluent B, 0.1% aqueous solution of CF_3COOH); retention time 26.7 and 27.1 min; for both peaks m/z = 1123 ($\text{M} - \text{CF}_3\text{COO}$), 505 ($(\text{M} - 2\text{CF}_3\text{COO})/2$).

Reaction of 1,1/*c,c*/DNP and 1,1/*t,t*/DNP with 9EtG. The reactions of the complexes 1,1/*c,c*/DNP, 1,1/*c,c*, 1,1/*t,t*/DNP, and 1,1/*t,t* (2 mM) with 2 equiv of 9EtG (4 mM) were monitored over 48 h at 310 K by ^1H NMR spectrometry in a mixture of D_2O and $\text{DMF}-d_7$ (1:1) in the case of 1,1/*c,c*/DNP and 1,1/*t,t*/DNP and in 0.1 M NaClO_4 D_2O solution (pD \sim 7.5) in the case of the label-free complexes. The pH titration of the products was subsequently performed by adjustment of pD with 0.1 and 1 M DCl and with 0.1 and 1 M NaOD without using a buffer. pD values were measured at 298 K using a PHM 80 pH meter (radiometer) before and after each ^1H NMR measurement. The pH values were corrected for the H/D isotope effect.⁵¹

Measurements of Platinum Accumulation in Cancer Cells. The 12-well culture plates containing exponentially growing U2-OS or U2-OS/Pt cells in Dulbecco's modified Eagle's medium (DMEM) supplemented with 10% fetal calf serum (Gibco, Paisley, Scotland), penicillin (100 units/mL, Duchefa, The Netherlands), and streptomycin (100 $\mu\text{g/mL}$, Duchefa, The Netherlands) (2×10^5 cells/well) were exposed to 20 μM of the labeled complexes (CFDA-Pt, DNP-Pt, 1,1/*c,c*/DNP, 1,1/*c,c*/CFDA, 1,1/*t,t*/CFDA, and 1,1/*t,t*/DNP) and the parent compounds (1,1/*c,c*, 1,1/*t,t*, and cisplatin) dissolved in DMEM for 30 min, 2 h, and 24 h (the complexes were added in duplicate). After incubation, the cells were washed twice with PBS, and 350 μL /well lysis buffer containing 10 mM Tris, pH 8.0, 150 mM NaCl, and 0.4% Triton X-100, was added. The content of each well was collected in an Eppendorf tube, and 100 μL of 10% SDS (sodium dodecyl sulfate) was added to each sample. After that, the samples were treated for 30 min at 50 °C with 20 $\mu\text{g/mL}$ of proteinase K (BV Sphaero Q, Gorinchem, The Netherlands). The samples were diluted with 20% HNO_3 to a final volume of 3 mL for measurement of platinum content. Platinum concentration was measured on a Varian Vista-MPX charge-coupled simultaneous ICP-OES (inductively coupled plasma optical emission spectrometer). The uptake experiments were carried out with duplicate cultures.

Cellular Processing Experiments. The U2-OS human osteosarcoma cell line (HTB 96, American Type Culture Collection) was originally derived from a sarcoma of the tibia. The cisplatin-resistant U2-OS/Pt cell line was kindly provided by Paola Perego of the Istituto Nazionale per lo Studio e la Cura dei Tumori, Milan, Italy. U2-OS cells and its cisplatin-resistant U2-OS/Pt cells were grown in Dulbecco's modified minimal essential medium without phenol red (Life Technologies) supplemented with 10% fetal bovine serum and antibiotics in a humidified 5% CO_2 , 95% air atmosphere. For living cell observations, the cells were plated in 35 mm culture dishes with a glass coverslip incorporated at the bottom (Mattek Corp. Ashland, MA), which is directly in contact with a 40 \times NA 1.30 oil-immersion objective (Neofluor) (Zeiss, Jena, Germany) during observations.

The cells were allowed to grow to 40–50% confluence before incubation. The CFDA-labeled compounds were diluted in serum-free medium and added to the cells at a final concentration of 10 μM . Then the cells were incubated for 30 min and subsequently washed with serum-free medium, and full growth medium was added to the cells, which were monitored over 48 h on an inverted microscope. The DNP-labeled compounds were observed after immunocytochemical staining (see below).

Immunocytochemical Staining of the DNP-Labeled Compounds. For immunohistochemical detection of the DNP-labeled compounds, the cells were fixed at different time points after internalization with 2% formaldehyde in CSK buffer (10 mM Pipes, pH 6.8, 300 mM sucrose, 100 mM NaCl, 3 mM MgCl_2 , 1 mM EGTA, 0.5% Triton X-100). In the fixation procedure, the cells were washed twice with PBS. The cells were fixed for 10 min at room temperature. Then the cells were washed twice with PBS before immunohistochemical staining.

After fixation, the cells were pretreated with 0.1% Triton X-100 in PBS for 15 min to improve target accessibility. The cells were then rinsed with TBS buffer (100 mM Tris-HCl, pH 7.5, 150 mM NaCl), incubated for 45 min with the primary antibody, a rabbit anti-DNP antibody (Sigma, St. Louis, Mo.), washed twice with TBS buffer, and incubated for 30 min with the secondary antibody, a goat anti-rabbit ALEXA 488 antibody (Molecular Probes, Leiden, The Netherlands). Antibody solutions were diluted in 100 mM Tris-HCl, 150 mM NaCl, and 0.5% blocking reagent (Boehringer). After the final washing steps, the cells were gradually dehydrated in an ethanol series of 70%, 90%, 100% for 1 min each. The coverslips were mounted in CytoFluor/DAPI (4,6-diamidino-2-phenylindole) for microscopic observation.

Golgi Staining. Staining of the Golgi complex was performed with *N*-([4-[4,4-difluoro-5-(2-thienyl)-4-bora-3a,4a-diaza-*s*-indacen-3-yl]phenoxy]acetyl)sphingosine (Bodipy-TR-ceramide, Molecular Probes, Leiden, The Netherlands). Twenty-four hours after incubation with 1,1/c,c/CFDA and 1,1/t,t/CFDA, Bodipy-TR-ceramide was added to the cells to a final concentration of 100 nM in serum-free medium. After 20 min of incubation with this dye, the cells were rinsed with serum-free medium and observed live using digital fluorescence microscopy. The CFDA-labeled complexes, emitting in green, and Bodipy-TR-ceramide, emitting red light, were sequentially visualized and digitally recorded.

Digital Fluorescence Microscopy. Fluorescence microscopy experiments were performed on a Axiovert 135 TV (Zeiss, Jena, Germany) inverted microscope equipped with a 100 W mercury arc lamp for fluorescence excitation and bright field illumination for phase contrast images. The filter set to detect CFDA fluorescence consisted of an hq 480/40 nm band-pass excitation filter, an hq 535/50 band-pass emitter filter, and a Q505 long-pass beam splitter. Bodipy-TR-ceramide was detected using a filter set composed of an hq 560/55 band-pass excitation filter, an hq 645/75 band-pass emitter filter, and a Q595 long-pass beam splitter. The temperature of the culture medium was controlled between 36 and 37 °C by a BIOPTECHS (Butler, PA) objective heater and a heated ring surrounding the culture chamber. Digital images were taken with a cooled CCD camera (Photometrix PLX, Tucson, AZ) using SCILL Image software (Multihouse, The Netherlands).

Growth Inhibition Assays in U2-OS and U2-OS/Pt Cells. Growth inhibition by the compounds was determined using an MTT-based assay (MTT, 3-(4,5-dimethylthiazol-2-yl)-2,5-diphenyl-2*H*-tetrazolium bromide).⁵² The U2-OS and U2-OS/Pt cells were grown as monolayers in Dulbecco's modified Eagle's medium (DMEM) supplemented with 10% fetal calf serum (Gibco, Paisley, Scotland), penicillin (100 units/mL, Duchefa, The Netherlands), and streptomycin (100 µg/mL, Duchefa, The Netherlands). After trypsinization, cells were divided in 96-well plates at concentrations of (3–5) × 10³ cells/well in 100 µL growth medium. The cells were allowed to attach overnight. After 24 h, fresh stock solutions (1 mg/mL) of 1,1/c,c, 1,1/t,t, and cisplatin in Millipore water and of the labeled compounds in dimethylformamide were diluted in medium. Five subsequent dilutions of each compound were added to the cells in quadruplicate, yielding a total volume of 200 µL in each well. Dimethylformamide diluted in medium at different concentrations (0.2–10%) was added to the cells in a control experiment. After 72 h of incubation, 50 µL of a 5 mg/mL MTT solution in PBS was added to each well and allowed to develop in the incubator (usually 120 min). After this, the medium was discarded and 100 µL of DMSO was added to each well, yielding purple solutions. The optical density was measured at 590 nm using a Biorad 550 microplate reader. The IC₅₀ values (drug concentration that inhibits cell growth for 50% with respect to control) were determined graphically using the Graphpad Prism analysis software package. In the cytotoxicity tests of the labeled complexes, dimethylformamide was added to the control cells.

Acknowledgment. The support from and sponsorship by COST Actions, Grant Nos. D20/0001/00, D20/

0002/00, and D20/0003/01 (Metal Compounds in the Treatment of Cancer and Viral Diseases), are kindly acknowledged. The authors are also indebted to a Training Network Grant from the EU in the 5th Framework program (MEDICINOR, Grant No. HPMT-CT-2000-00192). The authors thank Johnson & Matthey (Reading, U.K.) for their generous gift of K₂PtCl₄. This work was performed under the auspices of the joint BIOMAC Research Graduate School of Leiden University and Delft University of Technology.

Supporting Information Available: Results from elemental analysis for **2**, **4a**, **4b**, **6**, **7**, and **9** and HPLC spectra for **11a** and **11b**.

References

- (1) Farrell, N. Structurally novel platinum-based drugs in the clinic. Toward a new paradigm. *J. Inorg. Biochem.* **1999**, *74*, 23–23.
- (2) Komeda, S.; Kalayda, G. V.; Lutz, M.; Spek, A. L.; Yamanaka, Y.; Sato, T.; Chikuma, M.; Reedijk, J. New isomeric azine-bridged dinuclear platinum(II) complexes circumvent cross-resistance to cisplatin. *J. Med. Chem.* **2003**, *46*, 1210–1219.
- (3) Reedijk, J. New clues for platinum antitumor chemistry: Kinetically controlled metal binding to DNA. *Proc. Natl. Acad. Sci. U.S.A.* **2003**, *100*, 3611–3616.
- (4) Wong, E.; Giandomenico, C. M. Current status of platinum-based antitumor drugs. *Chem. Rev.* **1999**, *99*, 2451–2466.
- (5) Farrell, N.; Qu, Y.; Bierbach, U.; Valsecchi, M.; Menta, E. *Cisplatin: Chemistry and Biochemistry of a Leading Anticancer Drug*; Wiley VCH: Weinheim, Germany, 1999; pp 479–496.
- (6) Komeda, S.; Lutz, M.; Spek, A. L.; Chikuma, M.; Reedijk, J. New antitumor-active azole-bridged dinuclear platinum(II) complexes: Synthesis, characterization, crystal structures, and cytotoxic studies. *Inorg. Chem.* **2000**, *39*, 4230–4236.
- (7) Wheate, N. J.; Collins, J. G. Multi-nuclear platinum complexes as anti-cancer drugs. *Coord. Chem. Rev.* **2003**, *241*, 133–145.
- (8) Di Blasi, P.; Bernareggi, A.; Beggiolin, G.; Piazzoni, L.; Menta, E.; Formento, M. L. Cytotoxicity, cellular uptake and DNA binding of the novel trinuclear platinum complex BBR 3464 in sensitive and cisplatin resistant murine leukemia cells. *Anticancer Res.* **1998**, *18*, 3113–3117.
- (9) Manzotti, C.; Pratesi, G.; Menta, E.; Di Domenico, R.; Cavalletti, E.; Fiebig, H. H.; Kelland, L. R.; Farrell, N.; Polizzi, D.; Supino, R.; Pezzoni, G.; Zunino, F. BBR 3464: A novel triplatinum complex, exhibiting a preclinical profile of antitumor efficacy different from cisplatin. *Clin. Cancer Res.* **2000**, *6*, 2626–2634.
- (10) Rauter, H.; DiDomenico, R.; Menta, E.; Oliva, A.; Qu, Y.; Farrell, N. Selective platination of biologically relevant polyamines. Linear coordinating spermidine and spermine as amplifying linkers in dinuclear platinum complexes. *Inorg. Chem.* **1997**, *36*, 3919–3927.
- (11) Brabec, V.; Kasparkova, J.; Vrana, O.; Novakova, O.; Cox, J. W.; Qu, Y.; Farrell, N. DNA modifications by a novel bifunctional trinuclear platinum Phase I anticancer agent. *Biochemistry* **1999**, *38*, 6781–6790.
- (12) Mellish, K. J.; Qu, Y.; Scarsdale, N.; Farrell, N. Effect of geometric isomerism in dinuclear platinum antitumor complexes on the rate of formation and structure of intrastrand adducts with oligonucleotides. *Nucleic Acids Res.* **1997**, *25*, 1265–1271.
- (13) Johnson, A.; Qu, Y.; Van Houten, B.; Farrell, N. B-Z DNA conformational changes induced by a family of dinuclear bis-(platinum) complexes. *Nucleic Acids Res.* **1992**, *20*, 1697–1703.
- (14) Andrews, P.; Howell, S. Cellular pharmacology of cisplatin: perspectives on mechanisms of acquired resistance. *Cancer Cells* **1990**, *2*, 35–43.
- (15) Reedijk, J. Why does cisplatin reach guanine-N7 with competing S-donor ligands available in the cell? *Chem. Rev.* **1999**, *99*, 2499–2510.
- (16) Fuertes, M. A.; Alonso, C.; Perez, J. M. Biochemical modulation of cisplatin mechanisms of action: Enhancement of antitumor activity and circumvention of drug resistance. *Chem. Rev.* **2003**, *103*, 645–662.
- (17) Perez, R. P. Cellular and molecular determinants of cisplatin resistance. *Eur. J. Cancer* **1998**, *34*, 1535–1542.
- (18) Molenaar, C.; Teuben, J. M.; Heetebrij, R. J.; Tanke, H. J.; Reedijk, J. New insights in the cellular processing of platinum antitumor compounds, using fluorophore-labeled platinum complexes and digital fluorescence microscopy. *J. Biol. Inorg. Chem.* **2000**, *5*, 655–665.

- (19) Jansen, B. A. J.; Wielaard, P.; Kalayda, G. V.; Ferrari, M.; Molenaar, C.; Tanke, H. J.; Brouwer, J.; Reedijk, J. Dinuclear platinum complexes with *N,N'*-bis(aminoalkyl)-1,4-diaminoanthraquinones as linking ligands. Part I. Synthesis, cytotoxicity, and cellular studies in A2780 human ovarian carcinoma cells. *J. Biol. Inorg. Chem.* **2004**, *9*, 403–413.
- (20) Kalayda, G. V.; Jansen, B. A. J.; Molenaar, C.; Wielaard, P.; Tanke, H. J.; Reedijk, J. Dinuclear platinum complexes with *N,N'*-bis(aminoalkyl)-1,4-diaminoanthraquinones as linking ligands. Part II. Cellular processing in A2780 cisplatin-resistant human ovarian carcinoma cells: new insights into the mechanism of resistance. *J. Biol. Inorg. Chem.* **2004**, *9*, 414–422.
- (21) Kalayda, G. V.; Jansen, B. A. J.; Wielaard, P.; Tanke, H. J.; Reedijk, J. Dinuclear platinum anticancer complexes with fluorescent *N,N'*-bis(aminoalkyl)-1,4-diaminoanthraquinones: cellular processing in two cisplatin resistant cell lines reflects the differences in their resistance profiles. *J. Biol. Inorg. Chem.* **2005**, *10*, 305–315.
- (22) Arancia, G.; Calcabrini, A.; Meschini, S.; Molinari, A. Intracellular distribution of anthracyclines in drug resistant cells. *Cytotechnology* **1998**, *27*, 95–111.
- (23) Hindenburg, A. A.; Gervasoni, J. E., Jr.; Krishna, S.; Stewart, V. J.; Rosado, M.; Lutzky, J.; Bhalla, K.; Baker, M. A.; Taub, R. N. Intracellular distribution and pharmacokinetics of daunorubicin in anthracycline-sensitive and resistant HL-60 cells. *Cancer Res.* **1989**, *49*, 4607–4614.
- (24) Larsen, A. K.; Escargueil, A. E.; Skladanowski, A. Resistance mechanisms associated with altered intracellular distribution of anticancer agents. *Pharmacol. Ther.* **2000**, *85*, 217–229.
- (25) Meistermann, I.; Kalayda, G. V.; Hotze, A. C. G.; Reedijk, J. Preparation of a new ruthenium(II) building block for the synthesis of mixed-metal complexes. *Tetrahedron Lett.* **2004**, *45*, 2593–2596.
- (26) Yang, D. Z.; van Boom, S. S. G. E.; Reedijk, J.; van Boom, J. H.; Wang, A. H. J. Structure and isomerization of an intrastrand cisplatin-cross-linked octamer DNA duplex by NMR analysis. *Biochemistry* **1995**, *34*, 12912–12920.
- (27) Reedijk, J. Improved understanding in platinum antitumor chemistry. *Chem. Commun.* **1996**, 801–806.
- (28) Perego, P.; Caserini, C.; Gatti, L.; Carenini, N.; Romanelli, S.; Supino, R.; Colangelo, D.; Viano, I.; Leone, R.; Spinelli, S.; Pezzoni, G.; Manzotti, C.; Farrell, N.; Zunino, F. A novel trinuclear platinum complex overcomes cisplatin resistance in an osteosarcoma cell system. *Mol. Pharmacol.* **1999**, *55*, 528–534.
- (29) Declerck, L. S.; Bridts, C. H.; Mertens, A. M.; Moens, M. M.; Stevens, W. J. Use of fluorescent dyes in the determination of adherence of human leukocytes to endothelial cells and the effect of fluorochromes on cellular function. *J. Immunol. Methods* **1994**, *172*, 115–124.
- (30) Davenpeck, K. L.; Chrest, F. J.; Sterbinsky, S. A.; Bickel, C. A.; Bochner, B. S. Carboxyfluorescein diacetate labeling does not affect adhesion molecule expression or function in human neutrophils or eosinophils. *J. Immunol. Methods* **1995**, *188*, 79–89.
- (31) Perego, P.; Gatti, L.; Caserini, C.; Supino, R.; Colangelo, D.; Leone, R.; Spinelli, S.; Farrell, N.; Zunino, F. The cellular basis of the efficacy of the trinuclear platinum complex BBR 3464 against cisplatin-resistant cells. *J. Inorg. Biochem.* **1999**, *77*, 59–64.
- (32) Gong, Y. P.; Duvvuri, M.; Krise, J. P. Separate roles for the Golgi apparatus and lysosomes in the sequestration of drugs in the multi-drug resistant human leukemic cell line HL-60. *J. Biol. Chem.* **2003**, *278*, 50234–50239.
- (33) Bour-Dill, C.; Gramain, M. P.; Merlin, J. L.; Marchal, S.; Guillemin, F. Determination of intracellular organelles implicated in daunorubicin cytoplasmic sequestration in multidrug-resistant MCF-7 cells using fluorescence microscopy image analysis. *Cytometry* **2000**, *39*, 16–25.
- (34) Meijer, C.; de Vries, E. G. E.; Dam, W. A.; Wilkinson, M. H. F.; Hollema, H.; Hoekstra, H. J.; Mulder, N. H. Immunocytochemical analysis of cisplatin-induced platinum–DNA adducts with double-fluorescence video microscopy. *Br. J. Cancer* **1997**, *76*, 290–298.
- (35) Hall, M. D.; Dillon, C. T.; Zhang, M.; Beale, P.; Cai, Z.; Lai, B.; Stampfl, A. P. J.; Hambley, T. W. The cellular distribution and oxidation state of platinum(II) and platinum(IV) antitumor complexes in cancer cells. *J. Biol. Inorg. Chem.* **2003**, *8*, 726–732.
- (36) Jansen, B. A. J.; Brouwer, J.; Reedijk, J. Glutathione induces cellular resistance against cationic dinuclear platinum anticancer drugs. *J. Inorg. Biochem.* **2002**, *89*, 197–202.
- (37) Oehlsens, M. E. Q. Y.; Farrell, N. Reaction of polynuclear platinum antitumor compounds with reduced glutathione studied by multinuclear (^1H , ^1H – ^{15}N gradient heteronuclear single-quantum coherence, and ^{195}Pt) NMR spectroscopy. *Inorg. Chem.* **2003**, *42*, 5498–5506.
- (38) Roberts, J. D.; Peroutka, J.; Beggiolin, G.; Manzotti, C.; Piazzoni, L.; Farrell, N. Comparison of cytotoxicity and cellular accumulation of polynuclear platinum complexes in L1210 murine leukemia cell lines. *J. Inorg. Biochem.* **1999**, *77*, 47–50.
- (39) Center, M. S. Non-P-glycoprotein multidrug resistance in cell lines which are defective in the cellular accumulation of drug. *Cytotechnology* **1993**, *12*, 109–125.
- (40) Molinari, A.; Cianfriglia, M.; Meschini, S.; Calcabrini, A.; Arancia, G. P-glycoprotein expression in the Golgi apparatus of multidrug-resistant cells. *Int. J. Cancer* **1994**, *59*, 789–795.
- (41) Aggarwal, S. K. A Histochemical approach to the mechanism of action of cisplatin and its analogs. *J. Histochem. Cytochem.* **1993**, *41*, 1053–1073.
- (42) Edwards, P. G.; Kendall, M. D.; Morris, I. W. Effect of a platinum chemotherapy drug on intracellular elements during the cell cycle, using X-ray microanalysis. *Scanning Microsc.* **1991**, *5*, 797–810.
- (43) Olivero, O. A.; Semino, C.; Kassim, A.; Lopezlarraza, D. M.; Poirier, M. C. Preferential binding of cisplatin to mitochondrial DNA of Chinese hamster ovary. *Mutat. Res. Lett.* **1995**, *346*, 221–230.
- (44) Meijer, C.; van Luyn, M. J. A.; Nienhuis, E. F.; Blom, L.; Mulder, N. H.; de Vries, E. G. E. Ultrastructural morphology and localisation of cisplatin-induced platinum–DNA adducts in a cisplatin-sensitive and -resistant human small cell lung cancer cell line using electron microscopy. *Biochem. Pharmacol.* **2001**, *61*, 573–578.
- (45) Murata, T.; Hibasami, H.; Maekawa, S.; Tagawa, T.; Nakashima, K. Preferential binding of cisplatin to mitochondrial DNA and suppression of ATP generation in human malignant melanoma cells. *Biochem. Int.* **1990**, *20*, 949–955.
- (46) Giurgiovich, A. J.; Diwan, B. A.; Olivero, O. A.; Anderson, L. M.; Rice, J. M.; Poirier, M. C. Elevated mitochondrial cisplatin–DNA adduct levels in rat tissues after transplacental cisplatin exposure. *Carcinogenesis* **1997**, *18*, 93–96.
- (47) Kaufman, G. B.; Cowan, D. O. *Inorganic Synthesis*; McGraw-Hill Book Company, Inc.: New York, 1963; pp 242–243.
- (48) Qu, Y.; Farrell, N. Effect of diamine linker on the chemistry of bis(platinum) complexes—a comparison of the aqueous solution behavior of 1,4-butanediamine and 2,5-dimethyl-2,5-hexanediamine complexes. *J. Inorg. Biochem.* **1990**, *40*, 255–264.
- (49) Qu, Y.; Farrell, N. The product of the reaction of transdiamminedichloroplatinum(II) with diamines is dependent on chain length—example of a bridging ethylenediamine and formation of a novel trans-chelated structure with 1,5-pentanediamine. *Inorg. Chem.* **1992**, *31*, 930–932.
- (50) Farrell, N.; Appleton, T. G.; Qu, Y.; Roberts, J. D.; Fontes, A. P. S.; Skov, K. A.; Wu, P.; Zou, Y. Effects of geometric isomerism and ligand substitution in bifunctional dinuclear platinum complexes on binding properties and conformational changes in DNA. *Biochemistry* **1995**, *34*, 15480–15486.
- (51) Martin, R. B. Deuterated water effects on acid ionization constants. *Science* **1963**, *139*, 1198.
- (52) Alley, M. C.; Scudiero, D. A.; Monks, A.; Hursey, M. L.; Czerwinski, M. J.; Fine, D. L.; Abbott, B. J.; Mayo, J. G.; Shoemaker, R. H.; Boyd, M. R. Feasibility of drug screening with panels of human tumor cell lines using a microculture tetrazolium assay. *Cancer Res.* **1988**, *48*, 589–601.

JM050216H